Polyoxometalates

DOI: 10.1002/anie.200604180

Self-Patterning of Hydrophobic Materials into Highly Ordered Honeycomb Nanostructures at the Air/Water Interface**

Dawei Fan, Xiangfeng Jia, Peiqin Tang, Jingcheng Hao, and Tianbo Liu**

The patterning of functional materials into well-defined reproducible nanostructures with tunable sizes on incompatible surfaces is a challenging goal of both fundamental and practical importance. Herein, we report the unprecedented self-assembly of hydrophobic double-chain cationic surfactant hybrid materials DODMACl–$\{Mo_{72}Fe_{30}\}$ at the air/water interface, which leads to the formation of highly ordered honeycomb architectures. DODMACl is dioctadecyldimethylammonium chloride, $\{Mo_{72}Fe_{30}\}$ is the inorganic macroanion $Mo^{VI}_{72}Fe^{III}_{30}O_{252}L_{102}\cdot x\,H_2O$ ($x \approx 180$, $L = H_2O$, CH_3COO^-, $Mo_2O^{n-}_{8/9}$).

Recent progress in the synthesis of nanoscale polyoxometalate (POM) molecular clusters,[1] especially polyoxomolybdates and polyoxotungstates with well-defined structures and potential applications in catalysis, electrochemistry, biomedicine, and magnetism, as sensors, surfaces, and coatings,[1c,2] has successfully pushed the size of inorganic molecules to the nanometer scale, and offered new opportunities in many different fields. Some examples of water-soluble POMs are wheel-shaped $\{Mo_{154}\}$,[3] $\{Mo_{176}\}$,[4] and $\{Mo_{248}\}$,[5] C_{60}-like hollow spherical "Keplerate" $\{Mo_{132}\}$[6] and $\{Mo_{72}Fe_{30}\}$,[7] as well as the hedgehog-type cluster $\{Mo_{368}\}$.[8]

In this study, we use the 2.5-nm-diameter, C_{60}-like molecule $\{Mo_{72}Fe_{30}\}$ (Figure 1 A) as our model system. Many POMs are quite soluble in polar solvents because they contain a large number of water ligands and are negatively charged in solution (similar to polyelectrolytes), with the negative charge balanced by small counterions such as Na^+ and $NH_4{}^+$. $\{Mo_{72}Fe_{30}\}$ clusters are a little different. They exist as almost neutral molecules in crystals, but in solution they behave like a weak acid: the water ligands attached to the Fe^{III} centers tend to partially deprotonate, thus making $\{Mo_{72}Fe_{30}\}$ clusters slightly negatively charged (carrying several localized charges). The degree of deprotonation depends on the solution pH,[9] from almost 0 at pH 3.0 to 22 at pH 4.9. The hydrophilic POM surfaces can be adjusted to hydrophobic by forming surfactant-encapsulated clusters (SECs), through encapsulating the inorganic macroanions with a protective shell of water-soluble cationic species (such as surfactants) via electrostatic forces.[10] Many approaches have been developed to fabricate composite multilayers by electrostatic layer-by-layer self-assembly of POMs modified with a variety of water-soluble cationic species, including transition-metal complexes, cationic surfactants, polycations, and bipolar pyridine.[11] Recently, liquid-crystalline phases formed by ionic self-assembly of POM–surfactant complexes were also prepared.[12]

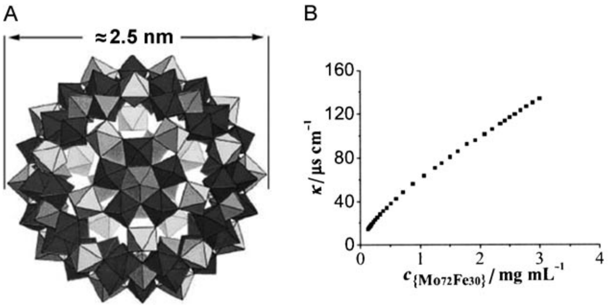

Figure 1. A) Structure of $\{Mo_{72}Fe_{30}\}$ "Keplerate" giant molecule. B) Conductivity data of aqueous solutions of $\{Mo_{72}Fe_{30}\}$ as a function of concentration.

For a 1.0 mg mL^{-1} $\{Mo_{72}Fe_{30}\}$ aqueous solution the pH is 3.4, which suggests that each $\{Mo_{72}Fe_{30}\}$ anion carries about seven net negative charges.[10d] The conductivity data, shown in Figure 1 B as a function of $\{Mo_{72}Fe_{30}\}$ concentration, clearly confirm that $\{Mo_{72}Fe_{30}\}$ is a weak electrolyte. Phase transfer of $\{Mo_{72}Fe_{30}\}$ from aqueous medium (upper phase) to a lower $CHCl_3$ phase can be achieved with the help of a certain amount of surfactant (DODMACl) dissolved in $CHCl_3$, which suggests that the concentration of DODMACl in $CHCl_3$ is critical to determining whether the $\{Mo_{72}Fe_{30}\}$ macroanions remain in the aqueous or $CHCl_3$ phase. If enough DODMACl is added, $\{Mo_{72}Fe_{30}\}$ can be transferred into the organic phase by forming $\{Mo_{72}Fe_{30}\}$–DODMA complexes through electrostatic interactions between the $\{Mo_{72}Fe_{30}\}$ anions and the $DODMA^+$ cations. The yellow color of the aqueous phase (from $\{Mo_{72}Fe_{30}\}$) continuously fades, while the color of the $CHCl_3$ phase turns gradually yellow. However, an excess amount of surfactant can form a second layer on the surface of complexes, with their hydrophilic polar heads facing outside, which makes the complexes relatively hydrophilic. Thus, the complexes in the $CHCl_3$ phase will be partially transferred back into the aqueous phase in the presence of an excess amount of surfactant.

Solvent-cast architectures of $\{Mo_{72}Fe_{30}\}$–DODMA complexes in organic medium were prepared at the air/water

---

[*] D. Fan, X. Jia, P. Tang, Prof. Dr. J. Hao
Key Laboratory of Colloid and Interface Chemistry of Ministry of Education, Shandong University
Jinan 250100 (P.R. China)
Fax: (+86) 531-8836-6074
E-mail: jhao@sdu.edu.cn
Prof. Dr. T. Liu
Department of Chemistry, Lehigh University
Bethlehem, PA 18015 (USA)
Fax: (+1) 610-758-6536
E-mail: til204@lehigh.edu

[**] This work was supported by the NSFC (20625307, 20571048, 20428101) and NSF (CHM0545983).

interface by evaporating $CHCl_3$, and were studied by transmission electron microscopy (TEM) using the method reported in the literature.[10a–c] We originally speculated that the fully hydrophobic complexes should spread homogeneously on the water surface, similar to the case of spreading a layer of oil at the air/water interface. However, in reality we found that the arrangement of complexes was very complicated and dependent on the concentration of DODMACl. When the DODMACl concentration is lower than $1.2\,mg\,mL^{-1}$ in $CHCl_3$, the architectures of $\{Mo_{72}Fe_{30}\}$–DODMA complexes at the air/water interface exhibit organized crystalline structures formed by the packing of the complexes. TEM observations reveal both monolayer (Figure 2 A) and multilayer (Figure 2 B and C) architectures with three-dimensionally ordered supramolecular structures spread over a broad area. The electron diffraction patterns (Figure 2, right column) confirm that these mono- and multilayer films are composed of complexes.

When the concentration of DODMACl reaches $1.2\,mg\,mL^{-1}$ in $CHCl_3$ ($c_{DODMACl} = 2.02\,mmol\,L^{-1}$; molar ratio of $\{Mo_{72}Fe_{30}\}$/surfactant $r \approx 1{:}90$), unique self-assembly of $\{Mo_{72}Fe_{30}\}$–DODMA complexes into microsized structures was observed. Typical TEM and HRTEM images are shown in Figure 3, obtained from solvent-cast films of $\{Mo_{72}Fe_{30}\}$–DODMA complexes at $c_{DODMACl} = 1.2\,mg\,mL^{-1}$ in $CHCl_3$.

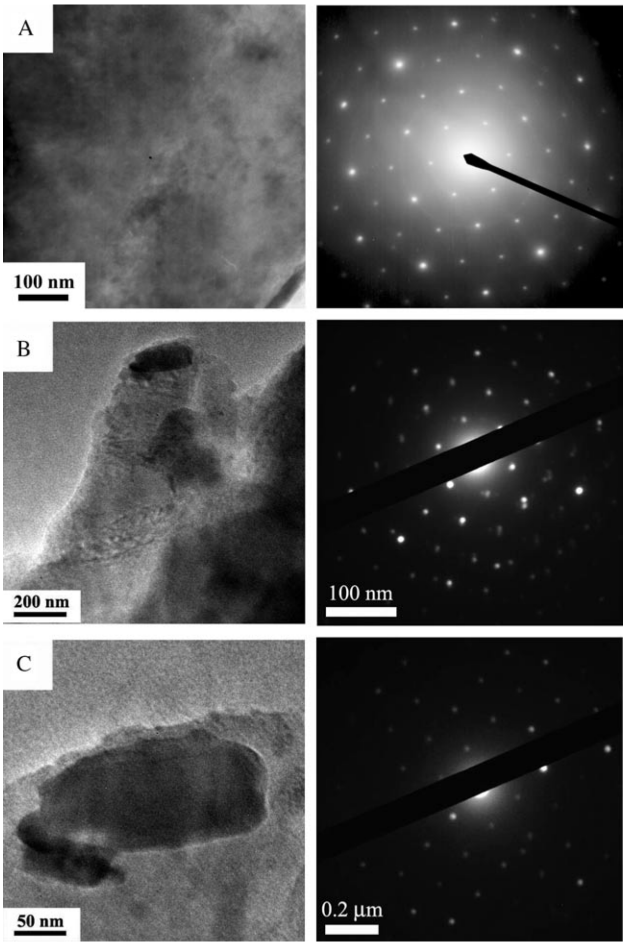

Figure 2. TEM images (left column) and the corresponding electron diffraction patterns (right column) of organized crystalline-structured monolayer films (A) and coexistent mono- and multilayer architectures (B) of $\{Mo_{72}Fe_{30}\}$–DODMA complexes. C) High-resolution TEM (HRTEM) image (left) and electron diffraction pattern (right) of organized crystalline-structured multilayer films.

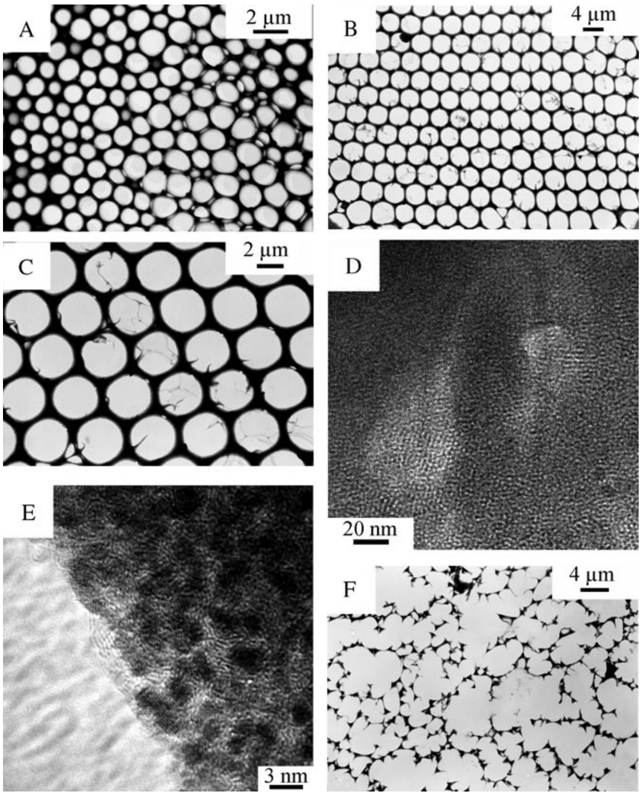

Figure 3. TEM images of A) $\{Mo_{72}Fe_{30}\}$–DODMA complexes at $c_{DODMACl} = 1.2\,mg\,mL^{-1}$ in $CHCl_3$; B, C) highly ordered honeycomb architectures of $\{Mo_{72}Fe_{30}\}$–DODMA complexes. D, E) HRTEM images of the highly ordered honeycombs, which reveal the ordered texture with $\{Mo_{72}Fe_{30}\}$ at $c_{DODMACl} = 2.0\,mg\,mL^{-1}$ in $CHCl_3$. F) TEM image of $\{Mo_{72}Fe_{30}\}$–DODMA complexes at $c_{DODMACl} = 4.0\,mg\,mL^{-1}$ in $CHCl_3$.

The thickness of the wall between pores is in general smaller than 0.5 μm and the pore sizes are not homogeneous, ranging from 0.5 to 1.5 μm (Figure 3 A). At $c_{DODMACl} = 2.0\,mg\,mL^{-1}$ ($c_{DODMACl} = 3.37\,mmol\,L^{-1}$ and $r \approx 1{:}150$), the nanostructure formed by $\{Mo_{72}Fe_{30}\}$–DODMA complexes (Figure 3 B and C) becomes highly ordered and porous, with honeycomb holes of uniform pore size (≈ 3.5 μm). The average thickness of the walls between the pores remains about 0.6 μm. HRTEM studies indicate that the walls are composed of many 2.5-nm-diameter dark objects (Figure 3 D and E) that can be attributed to single $\{Mo_{72}Fe_{30}\}$ clusters. This result confirms that the $\{Mo_{72}Fe_{30}\}$ clusters play a critical role in constructing the uniform honeycomb structures, together with the surfactant. Scanning electron microscopy (SEM) of the same system confirms the porous structure (Figure 4). In particular, it shows that small holes exist inside the 500-nm-thick walls.

When the concentration of DODMACl is higher than $4.0\,mg\,mL^{-1}$ in $CHCl_3$ ($c_{DODMACl} = 6.73\,mmol\,L^{-1}$ and $r \approx 1{:}300$; see Figure 3 F), the unique honeycomb structures

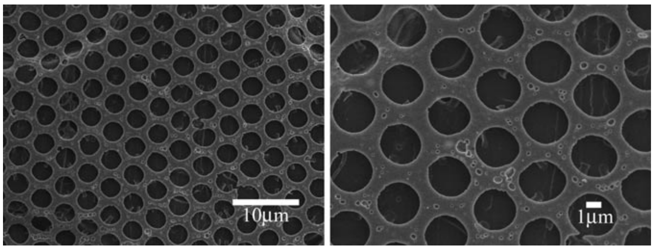

Figure 4. SEM images of highly ordered honeycomb architectures of $\{Mo_{72}Fe_{30}\}$–DODMA complexes.

are not observed any more. In summary, the formation of highly ordered patterns formed by complexes heavily depends on the surfactant concentration, given the fixed $\{Mo_{72}Fe_{30}\}$ concentration in aqueous solution. If the amount of surfactant is low (barely enough to cover the POM macroanions and form complexes), regular close-packing of spherical complexes is observed. With increasing surfactant concentration, the free-energy-favored patterning structure gradually becomes the unique honeycomb structure. This structure first appears to have polydispersed pores (Figure 3A), then the pores become more uniform and the packing of pores becomes more ordered with increasing surfactant concentration until an optimum is achieved (Figure 3B–E). In the presence of excess surfactant, the highly ordered patterns become a disordered structure again. This could be because excess surfactant will make the complexes more hydrophilic. The relatively hydrophilic complexes have a higher affinity to the water phase, so they cannot form ordered patterns at the air/water interface.

Figure 5A shows the ^{1}H NMR spectrum of DODMACl in $CDCl_3$ solution. The peaks are very sharp and each group of protons on DODMACl can be readily identified. Figure 5B shows the ^{1}H NMR spectrum of $\{Mo_{72}Fe_{30}\}$–DODMA complex in $CDCl_3$ at $c_{DODMACl} = 2.0$ mg mL^{-1}. The α-CH_2, β-CH_2, and ω′-CH_3 resonances become very weak as a result of the strong electrostatic interaction between the DODMA$^+$ cations and $\{Mo_{72}Fe_{30}\}$ anions, which changes the chemical environments of these moieties. In Figure 5C (complexes in $CDCl_3$ solution at $c_{DODMACl} = 8.0$ mg mL^{-1}), the peaks arising from α-CH_2, β-CH_2, and ω′-CH_3 reappear because of the excess surfactant, but are much broader than those in Figure 5A (on account of the electrostatic interaction between surfactant and $\{Mo_{72}Fe_{30}\}$).

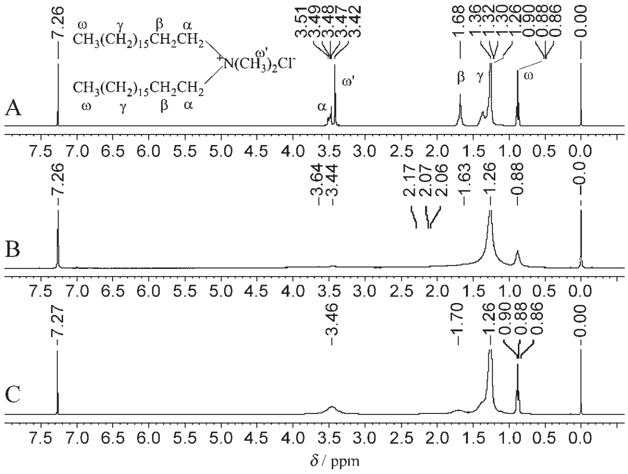

Figure 5. ^{1}H NMR spectra of A) DODMACl in $CDCl_3$, and $\{Mo_{72}Fe_{30}\}$–DODMA in $CDCl_3$ at B) $c_{DODMACl} = 2.0$ and C) 8.0 mg mL^{-1}.

The above results show that the DODMA$^+$ cations encapsulate the $\{Mo_{72}Fe_{30}\}$ anions effectively at $c_{DODMACl} = 2.0$ mg mL^{-1}. When the hydrophobic $\{Mo_{72}Fe_{30}\}$–DODMA complexes are transferred into the air/water interface, they should shrink in volume to minimize the free energy,[13] that is, to minimize surface tension. The shape of the self-assembled structures at the air/water interface should be the optimal topology. In our current case, with $c_{DODMACl} = 2.0$ mg mL^{-1} in $CHCl_3$, honeycomb architectures seem to be the optimal morphology with the minimum surface energy. Another possible explanation of the honeycomb structure is that the evaporation of organic solvent ($CHCl_3$) at the air/water interface leads to the condensation of vapor in air into microscale water beads, which result in micropores after drying, as discovered by François et al.[14] We notice that our current experimental conditions are different, and more studies are needed to elucidate the mechanism of formation of the honeycomb structure. At the moment, we can at least claim that this is a novel way of fabricating highly ordered porous structures at the air/water interface, with incorporation of a large amount of functional inorganic material homogeneously into the walls of the pores.

In summary, the $\{Mo_{72}Fe_{30}\}$–DODMA complexes produced in $CHCl_3$ form patterns with highly ordered and uniform structures at the air/water interface after evaporation of the organic solvent. The concentration of DODMACl in $CHCl_3$ is critical. We are working on other POMs, such as $\{Mo_{132}\}$, to test the generality of these observations. The formation of highly ordered, uniform, reproducible nanopores at an interface, with homogeneously incorporated inorganic materials, might find various potential applications, such as the development of new materials for catalysis, separation membranes, microstructured electrode surfaces, nanocontainers, or nanoreactors.

Experimental Section

$\{Mo_{72}Fe_{30}\}$ was synthesized according to the literature.[6,7] A series of solutions of DODMACl (0–20 mg mL^{-1}) in $CHCl_3$ (5.0 mL) were mixed with an aqueous solution of $\{Mo_{72}Fe_{30}\}$ (1.0 mg mL^{-1}, 5.0 mL). Subsequently, the samples were sonicated at 100 W for 5 min and equilibrated at 25.0 ± 0.1 °C for 1 month. An amount of $CHCl_3$-phase solution was dropped onto a pure water surface; the solvent-cast architectures of $\{Mo_{72}Fe_{30}\}$–DODMA complexes formed after evaporating $CHCl_3$ were studied by TEM observations.[10a–c] The highly ordered honeycomb superstructures of $\{Mo_{72}Fe_{30}\}$–DODMA complexes in $CHCl_3$ were obtained at an acceleration voltage of 100 kV (JEM-100 CXIII, JEOL). HRTEM images were observed at an acceleration voltage of 200 kV (JEM-2010, JEOL). SEM images were obtained with a JEOL JSM6700F field-emission scanning electron microscope. Three samples were prepared and equilibrated for 1 month at 25.0 ± 0.1 °C: 1) DODMACl in $CDCl_3$ (2.0 mg mL^{-1}); and $\{Mo_{72}Fe_{30}\}$ (1.0 mg mL^{-1}) in D_2O (5.0 mL) mixed with 2) 2.0 and 3) 8.0 mg mL^{-1} DODMACl in $CDCl_3$ (5.0 mL). The organic phase ($CDCl_3$) was examined by ^{1}H NMR spectroscopy in 5-mm tubes. A

Bruker AM-400 spectrometer was used for the ^{1}H NMR measurements at 25.0 ± 0.1 °C.

Received: October 12, 2006
Revised: December 15, 2006

Keywords: microporous materials · phase transitions · polyoxometalates · self-assembly · surfactants

---

[1] a) A. Müller, C. Serain, *Acc. Chem. Res.* **2000**, *33*, 2–10; b) A. Müller, M. Henry, *C. R. Chim.* **2003**, *6*, 1201–1208; c) L. Cronin in *Comprehensive Coordination Chemistry II*, *Vol. 7* (Eds.: J. A. McCleverty, T. J. Meyer), Elsevier, Amsterdam, **2004**, pp. 1–56; d) *Polyoxometalate Molecular Science: From Biology to Nanotechnology* (Eds.: J. J. Borrás-Almenar, E. Coronado, A. Müller, M. T. Pope), Kluwer, Dordrecht, **2003**.

[2] N. Casañ-Pastor, P. Gómez-Romero, *Front. Biosci.* **2004**, *9*, 1759–1770.

[3] A. Müller, S. K. Das, V. P. Fedin, E. Krickemeyer, C. Beugholt, H. Bögge, M. Schmidtmann, B. Hauptfleisch, *Z. Anorg. Allg. Chem.* **1999**, *625*, 1187–1192.

[4] A. Müller, M. Koop, H. Bögge, M. Schmidtmann, C. Beugholt, *Chem. Commun.* **1998**, *15*, 1501–1502.

[5] A. Müller, S. Q. N. Shah, H. Bögge, M. Schmidtmann, *Nature* **1999**, *397*, 48–50.

[6] A. Müller, E. Krickemeyer, H. Bögge, M. Schmidtmann, F. Peters, *Angew. Chem.* **1998**, *110*, 3567–3571; *Angew. Chem. Int. Ed.* **1998**, *37*, 3359–3363.

[7] A. Müller, S. Sarkar, S. Q. N. Shah, H. Bögge, M. Schmidtmann, S. Sarkar, P. Kögerler, B. Hauptfleisch, A. X. Trautwein, V. Schünemann, *Angew. Chem.* **1999**, *111*, 3435–3439; *Angew. Chem. Int. Ed.* **1999**, *38*, 3238–3241.

[8] a) A. Müller, E. Beckmann, H. Bögge, M. Schmidtmann, A. Dress, *Angew. Chem.* **2002**, *114*, 1210–1215; *Angew. Chem. Int. Ed.* **2002**, *41*, 1162–1167; b) A. Müller, B. Botar, S. K. Das, H. Bögge, M. Schmidtmann, A. Merca, *Polyhedron* **2004**, *23*, 2381–2385.

[9] T. Liu, B. Imber, E. Diemann, G. Liu, K. Cokleski, H. Li, Z. Chen, A. Müller, *J. Am. Chem. Soc.* **2006**, *128*, 15914–15920.

[10] a) D. G. Kurth, P. Lehmann, D. Volkmer, H. Cölfen, M. J. Koop, A. Müller, A. Du Chesne, *Chem. Eur. J.* **2000**, *6*, 385–393; b) D. Volkmer, A. Du Chesne, D. G. Kurth, H. Schnablegger, P. Lehmann, J. Koop, A. Müller, *J. Am. Chem. Soc.* **2000**, *122*, 1995–1998; c) D. G. Kurth, P. Lehmann, D. Volkmer, A. Müller, D. Schwahn, *J. Chem. Soc. Dalton Trans.* **2000**, 3989–3998; d) T. Liu, *J. Cluster Sci.* **2003**, *14*, 215–226; e) W. Bu, H. Li, H. Sun, S. Yin, L. Wu, *J. Am. Chem. Soc.* **2005**, *127*, 8016–8017; f) W. Bu, H. Li, W. Li, L. Wu, C. Zhai, Y. Wu, *J. Phys. Chem. B* **2004**, *108*, 12776–12782.

[11] a) S. Liu, D. Volkmer, D. G. Kurth, *J. Cluster Sci.* **2003**, *14*, 405–419; b) D. G. Kurth, D. Volkmer, M. Ruttorf, B. Richter, A. Müller, *Chem. Mater.* **2000**, *12*, 2829–2831.

[12] a) T. Zhang, C. Spitz, M. Antonietti, C. F. J. Faul, *Chem. Eur. J.* **2005**, *11*, 1001–1009; b) S. Polarz, B. Smarsly, M. Antonietti, *ChemPhysChem* **2001**, *2*, 457–461.

[13] M. Srinivasarao, D. Collings, A. Philips, S. Patel, *Science* **2001**, *292*, 79–83.

[14] a) G. Widawski, B. François, *Nature* **1994**, *369*, 387–389; b) B. François, O. Pitois, J. François, *Adv. Mater.* **1995**, *7*, 1041–1044; c) O. Pitois, B. François, *Eur. Phys. J. B* **1999**, *8*, 225–231; d) O. Pitois, B. François, *Colloid Polym. Sci.* **1999**, *277*, 574–578.